

Phase Unwrapping Techniques for SRTM

C. L. Werner, R. M. Goldstein, S. Hensley, P. A. Rosen, E. Chapin

Jet Propulsion Laboratory 4800 Oak Grove Drive, Pasadena CA, USA 91104

Tel: 1.818.354.0463 email: cw@vega.nasa.jpl.gov

The Shuttle Radar Topographic Mission will map 80% of the Earth land mass topography with one arc-sec (30 meter) posting using a 60 meter baseline radar interferometer. The mosaicked DTED level-2 map products will have 10 meter relative and 16 meter absolute height resolution at the 90% percent level. The radar will operate in a 4-beam SCAN-SAR mode using two sets of beams with orthogonal polarizations. On-board tape recorders will archive over 6.5 Tb of C-Band data. Within 1 year these data will be reduced to mosaicked map products.

The sheer volume of data necessitates that the phase unwrapping algorithm for the interferograms be robust and rapid. It must be able to operate in a continuous strip mapping mode, since many acquisitions are continental in scale. The Topography Processing System (TPS) produces Single Look Complex (SLC) images from echoes acquired from both the in-board and out-board antennas and forms single-look interferograms on a burst by burst basis. Every point in the swath will be illuminated by between 2 and 3 bursts. Interferograms from each of the bursts with approximately 50 lines will be combined to form patches of about 3000 lines each for block processing of the image strips.

The phase values of the multi-look interferograms are modulo 2π . Phase unwrapping consists of determining the correct multiple of 2π to add to each point in the interferogram such that integration of the phase between any two points is path independent. Phase differences between the pixels are summed assuming that the magnitude difference is less than π along the integration path. Radar interferograms pose characteristics that complicate this simple approach. Decorrelation caused by thermal noise, surface geometry, shadow and layover corrupt the phase values introducing inconsistencies that prevents simple integration. The integration paths must be restricted such that the integral is independent of the path chosen within the restricted set. Restriction of the path is done by placing "cuts" in the image plane that the integration cannot cross.

1 Branch Cut Unwrapping

The SRTM algorithm for creation of the cuts is a modification of the branch cut algorithm introduced by Goldstein [1]. It recognizes that inconsistencies in the phase are local. Summation of the phase differences around a closed path taking the closest multiple of 2π gives an inconsistent result around these points, which are termed "residues". Positive residues have a residual "charge" of $+2\pi$ and negative residues -2π for a clockwise path. Connection of the residues by "branch" cuts to create neutralized "trees" localizes the phase jumps to occur across the cuts. Ideally these branches lie in regions that will be excluded from unwrapping. The algorithm, as originally proposed, begins by searching for an unvisited residue to form the start of a tree. A sequential search following this searches around each of the tree residues drawing cuts to other residues until the tree is neutralized. At each stage the region surrounding each residue is searched up to a certain distance. Once all the residues in the current tree have been searched, the size of the search distance is increased and areas around all members of the tree are rescanned. This process continues until the tree is neutralized, or the size of the search region exceeds a predetermined bound. When the algorithm is finished with a tree, it searches for a new unvisited residue, and the process of growing a tree repeats. The edges of the patch are problematical because the residue structure is unknown beyond the edge. Connections to the edge to discharge a tree are permitted after the size of the search region exceeds a specified threshold. The unwrapped phase close to the edge may contain small residual errors because the cut was arbitrarily drawn.

The algorithm effectively excludes regions of high residue density related to low SNR or layover by creating a dense network of interlocking cuts. These regions may also be excluded by estimation of the correlation coefficient and setting a threshold for unwrapping. Once the phase unwrapping trees have been constructed, the phase is unwrapped by simple integration of the phase differences. A region growing algorithm is used to perform the integra-

tion and rapidly fills the image plane beginning at a single point called a “seed”.

1.1 Neutrons

Localization of the phase discontinuities through the use of branch cuts does not have a unique solution. There are many ways to connect the residues, but which is best? Criteria have been proposed including minimization of the total length of branch cuts [2], but this in practice is not optimal because it ignores the physical characteristics of the SAR images. As stated before, the two main difficulties facing SAR unwrapping algorithms are regions of shadow and layover. Madsen suggested the use of non-charged points (neutrons), that act as residues to guide tree growth, but do not affect the net tree charge [3]. Neutrons do not contribute to the total charge of the current tree, but serve to reduce the size of the search region. Placing neutrons in regions of layover encourages the growth of branches in those areas. Algorithms have been proposed for the deployment of neutrons based upon the second derivative of the phase [4], the phase gradient, and radar backscatter intensity. All of these methods aim to localize the branch cuts to lie within areas that are prone to unwrapping errors or where the correlation is low. The current approach uses SAR backscatter to determine the neutron locations by comparing the intensity of each pixel to a threshold. The threshold is chosen to generate a fixed percentage of neutrons regardless of contrast in the scene. In high contrast scenes the neutrons will congregate in layover regions, and improve tree structure by reducing the overall maximum length of cuts.

1.2 Connected Components

Continuous phase unwrapping from one patch to the next has been implemented using a connected components algorithm. Continuous unwrapping of long image strips proceeds by saving the unwrapped phase along a line in the previous patch (the bootstrap line). Locations along this line are matched to the corresponding locations in the current patch. Due to changes in the processing parameters, unwrapped phase values along the bootstrap line of the previous patch may differ from values along the matching points in the current patch. The unwrapped phase values along the bootstrap phase line must be adjusted to account for changes in processing such as doppler centroid. Furthermore, mapping from one patch to the next may involve a range dependent azimuth shift. Seed points are chosen from points along the line. After unwrapping, phase values along the bootstrap line are compared with the newly unwrapped values to determine the nearest multiple of 2π . The variance of

the phase is also evaluated to test for unwrapping errors. If the variance exceeds a threshold, points in the unwrapped region are rejected and unwrapping proceeds starting from another seed. A correlation threshold is used to exclude regions to reduce unwrapping errors. If after all the seeds are exhausted and an insufficient fraction of the image has been unwrapped correctly, the correlation threshold is raised incrementally to reduce global errors at the expense of unwrapping a smaller fraction of the patch.

2 Adaptive Filtering

The interferogram power spectrum is characterized by a narrow band component associated with the fringe spectrum and a broadband noise component. The local fringe phase shift, $\delta\phi$, per slant range pixel, δr , is a function of the local incidence angle, θ , radar slant range, ρ , and perpendicular baseline component, B_{perp} :

$$\delta\phi = \frac{4\pi}{\lambda} \frac{B_{\perp} \delta r}{\rho \tan(\theta - \xi)}. \quad (1)$$

A new filtering algorithm has been developed that uses the interferometric data to estimate the fringe power spectrum and derive a filter from this spectrum [5]. The advantage of this algorithm is that it is adaptive to the slope dependent fringe spectrum. The image is divided into overlapping patches and a periodogram estimate of the power spectrum is obtained by smoothing the detected 2-dimensional Fourier transform of the windowed patch. The adaptive filter $Z(\omega_x, \omega_y)$ is derived from the smoothed power spectrum $\tilde{S}(\omega_x, \omega_y)$ by the operation:

$$Z(\omega_x, \omega_y) = \left| \tilde{S}(\omega_x, \omega_y) \right|^{\alpha}, \quad (2)$$

where the exponent α lies typically in the range of $[0, 1.0]$. A value of 0 performs no filtering while an exponent of 1.0 applies narrow-band filtering to the scene. Given a Gaussian shaped fringe power spectrum and filter $\alpha = 1$, the signal band-area is halved and the signal to noise ratio is squared in the filtered interferogram. Discontinuities in the phase between overlapping patches are minimized by weighting the filter output with a triangular window and summing the values. The filter bandwidth is a non-linear function of the local fringe spectrum and coherence. The adaptive bandwidth characteristic of this algorithm strongly filters regions with high coherence and little variation in the phase associated with regions of low relief. In contrast, regions of pure noise remain unsmoothed. From a phase unwrapping aspect, the residue density before and after filtering remains about the same in

uncorrelated regions. The high residue density in these areas prevents unwrapping these regions of low SNR.

Selection of the exponent α is optimized for the simulated data by minimization of the phase standard deviation σ_ϕ relative to the true phase. An increased value of the exponent reduces the effective filter bandwidth, reducing phase noise at the cost of degraded resolution and loss of topographic features. Therefore, the optimum will be dependent on the roughness of the local topography with mountainous regions requiring smaller values of the exponent relative smooth areas.

3 Unwrapping Simulation

The goal of the unwrapping algorithm is to maximize the total number of pixels unwrapped correctly, while minimizing the percentage of errors. One type of error occurs when an area has been assigned the wrong multiple of 2π but should have been unwrapped correctly by the algorithm. Another kind of error occurs when unwrapping has taken place of a region without meaningful height information such as layover or shadow or is a region that is not connected to the rest of the interferogram.

Our approach to test the accuracy of the unwrapping algorithm is to simulate interferometric data using real topography derived from the NASA/JPL TOPSAR instrument [6, 7]. The simulator divides the surface into small scattering elements with Lambertian scattering. The complex field contributions to the signal at each of the antennae from each of the scatterers are then summed. The simulated interferogram pixel is created by summing the single look interferogram samples derived by interfering the simulated SLC values. The simulation effectively models phase differences associated with the interferometer and imaging geometry, temporal decorrelation, thermal noise, and the number of interferometric looks [8, 9]. Thermal noise is added to the SAR signal such that the SNR of 12 dB over flat terrain matches the predicted SRTM SNR at the 90% confidence level.

The simulator creates maps of layover and shadow, absolute phase without noise, radar backscatter intensity for each of the two antennas, and the simulated multi-look interferogram. After unwrapping, the phase is compared with the true phase to determine the nearest multiple of 2π in phase difference. Unwrapping errors often occur on the edges of shadow and layover are called embayments in our terminology. The percentages of correctly unwrapped pixels, the errors, and the type of error are then evaluated.

Simulated SRTM interferograms were created

PARAMETER	38.0 deg. (percent)	53.5 deg. (percent)
layover pixels:	0.09828	0.00100
shadow pixels:	0.03150	2.54452
residues:	0.14891	0.73647
neutrons:	0.19946	0.09799
unwrapped pixels:	97.48068	95.67370
embayments (shadow):	0.00000	0.00002
embayments (layover):	0.01221	0.00093
embayments (total):	0.01221	0.00095
errors(no shadow/layover):	0.00498	0.00002
blunders (total errors):	0.01719	0.00098
mean σ_ϕ :	7.561	7.417

Table 1: Unwrapping statistics for the $2K \times 2K$ simulated SRTM interferograms Incidence angles correspond to the inner and outer SRTM image swaths.

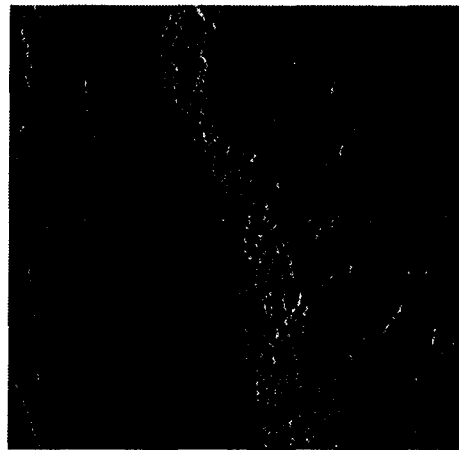


Figure 1: Simulated SRTM interferogram, 38.0 degrees incidence angle at center swath. The phase is mapped as 2π per fringe.

from topographic data acquired by the TOPSAR merged with USGS data to fill gaps over the White Mountains in California and decimated to 25 meter posting approximating the SRTM geometry. This area was selected because it is very rugged and contains both layover and shadow when imaged. Regions of SRTM interferograms were simulated with a size of 2048×2048 for the inner (38 degrees incidence angle) and outer swaths (53.5 degrees incidence angle) as shown in Fig.1 and Fig.2. A total of 2 looks for each interferogram sample was generated. Unwrapping performance using the adaptive interferogram filter with a exponent of 0.2 and Correlation threshold of 0.5 are summarized in Table 1.

A sample of the residues, neutrons, low correlation, and branch cuts is shown in Fig. 3 for a small region in the simulated interferogram with 53.5 degree incidence angle. Note how the low correlation mask encloses the regions of shadow that have high phase noise.

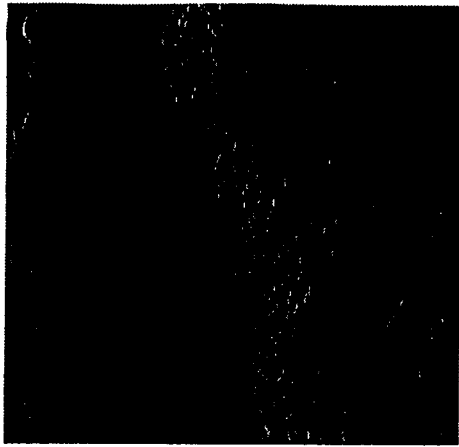


Figure 2: Simulated SRTM interferogram, 53.5 degrees incidence angle at center swath. The phase is mapped as 2π per fringe.

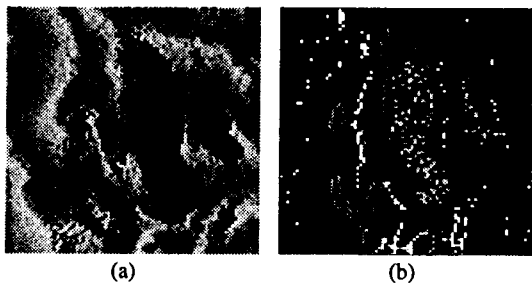


Figure 3: Simulated interferometric phase and the associated unwrapping flags. The unwrapping flags are coded as follows: red: + residue, blue: - residue, white: neutron, yellow: branch cut, tan: low correlation).

4 Conclusions

The branch cut algorithms are very effective for unwrapping the phase of the SRTM mission. Error rates predicted from the simulation will be less than 0.02% for the inner beam, decreasing to less than 0.001% for the outer beam. Errors come about mostly by unwrapping into regions of layover rather than into shadow regions.

Acknowledgments

This work was performed at the Jet Propulsion Laboratory, California Institute of Technology under contract with NASA as part of the SRTM project.

References

[1] Goldstein, R. M., H. A. Zebker, and C. L. Werner, Satellite radar interferometry: Two-

dimensional phase unwrapping. *Radio Science* 23, 713-720, 1988.

- [2] Costantini, M., Validation of a novel phase unwrap algorithm using true and simulated ERS tandem SAR interferometric data, Proceedings of the 3rd ERS symposium, Florence, Italy, 1997.
- [3] Madsen, S. N., and P. A. Rosen, Proceedings of the Interferometric SAR Technology and Applications Symposium, Ft. Belvoir, VA, 159-178, 1993.
- [4] Bone, D. J., Fourier fringe analysis-the 2-dimensional phase unwrapping problem, *Applied Optics*, 30, 3627-3632, 1991.
- [5] Goldstein, R. M., and C. L. Werner, Radar Interferogram Filtering for Geophysical Applications, submitted to Geophysical Research Letters March, 1998.
- [6] Zebker, H. A., S. N. Madsen, J. M. Martin, K. B. Wheeler, T. Miller, Y. Lou, G. Alberti, S. Vetrilla, and A. Cucci, The TOPSAR interferometric radar topographic mapping instrument, *IEEE Trans. Geoscience and Remote Sensing*, 30, 933-940, 1992.
- [7] Madsen, S. N., J. M. Martin, and H. A. Zebker, Topographic mapping using radar interferometry: Processing techniques, *IEEE Trans. Geoscience and Remote Sensing*, 31, 246-256, 1993.
- [8] Li, F. K. and R. M. Goldstein, Studies of multi-baseline space-borne interferometric synthetic aperture radars, *IEEE Trans Geoscience and Remote Sensing*, 28, 88-97, 1990.
- [9] Zebker, H. A., and J. Villasenor, Decorrelation in interferometric radar echoes, *IEEE Trans Geoscience and Remote Sensing*, 30, 950-959, 1992.